Afyon Kocatepe Üniversitesi Fen ve Mühendislik Bilimleri Dergisi
Afyon Kocatepe University – Journal of Science and Engineering
https://dergipark.org.tr/tr/pub/akufemubid

Araştırma Makalesi / Research Article
e-ISSN: 2149-3367
DOI: https://doi.org/10.35414/akufemubid.1880940
CITE: Afyon Kocatepe University Journal of Science and Engineering 26(3) (2026) 751-760

Spark Plasma Sintered B_4C-Based Composites with WC and Y_2O_3 Additives: Phase Evolution, Densification and Microstructural Analysis

*Makale Bilgisi / Article Info
Alındı/Received: 05.02.2026
Kabul/Accepted: 25.04.2026
Yayımlandı/Published: 03.06.2026

WC ve Y_2O_3 Katkılı Spark Plazma Sinterlenmiş B_4C Bazlı Kompozitler: Faz Gelişimi, Yoğunlaşma ve Mikro Yapı Analizi

Pelin Çağım TOKAT-BİRGİN*, Hediye AYDIN

Kütahya Dumlupınar University, Department of Metallurgy and Material Engineering, Kütahya, Türkiye

Abstract

B_4C matrix composites were produced using the spark plasma sintering (SPS) method at a temperature of 1900°C and a pressure of 40 MPa. In the production process, WC additives at volumes of 15%, 17.5%, and 20% and Y_2O_3 additives at volumes of 2.5% and 5% were used. The mechanical properties of composites produced using the SPS method have been investigated in relation to the effect of secondary phases on the structure. The sintered ceramic matrix composites exhibited a high fracture toughness of 8.1 MPa· $m^{1/2}$ and a Vickers hardness of 23.5 GPa. This remarkable improvement is attributed to the reduction in grain size, the formation of secondary phases, and energy loss mechanisms resulting from fracture along grain boundaries.

Keywords *Boron Carbide (B_4C), Ceramic Matrix Composite (CMC), Spark Plasma Sintering (SPS), Mechanical Properties*

Öz

B_4C matris kompozitler, 1900 °C sıcaklık ve 40 MPa basınçta spark plazma sinterleme (SPS) yöntemi kullanılarak üretilmiştir. Üretim sürecinde, hacimce %15, %17,5 ve %20 oranlarında WC ve hacimce %2,5 ve %5 oranlarında Y_2O_3 katkıları kullanılmıştır. SPS yöntemi kullanılarak üretilen kompozitlerin mekanik özellikleri, ikincil fazların yapı üzerindeki etkisi ile ilişkili olarak incelenmiştir. Sinterlenmiş seramik matris kompozitler, 8.1 MPa· $m^{1/2}$'lik yüksek bir kırılma tokluğu ve 23.5 GPa'lık bir Vickers sertliği sergilemiştir. Bu dikkate değer iyileşme, tane boyutunun küçülmesi, ikincil fazların oluşumu ve tane sınırları boyunca kırılmadan kaynaklanan enerji kaybı mekanizmalarına atfedilebilir.

Anahtar Kelimeler *Bor Karbür (B_4C), Seramik Matris Kompozit (CMC), Spark Plazma Sinterleme (SPS), Mekanik Özellikler*

1. Introduction

Boron carbide (B_4C) is selected for high-performance applications because of its great hardness, low density, high melting point, excellent neutron absorption capacity, and good thermoelectric properties (Zhang et al., 2019). Cutting tools coated with boron carbide can be used for cutting various alloys including brass, stainless steel, titanium, aluminum, and cast iron. The sintered product form also has applications in spray nozzles and ceramic bearings as well as wire drawing dies due to its excellent wear resistance (Shin et al., 2023; Schmidt, 2023). It is also utilized where vehicle armoring is required because of the combination of low density with high hardness plus impact resistance (Wu et al., 2020). Boron carbide thin film coatings have found application as a protective coating in the electronic industry (Chen et al., 2006). It has been extensively used in nuclear reactors as a control rod material for protection as well as a neutron detector because it absorbs neutrons without creating long-lived radionuclides. Boron carbide's neutron absorption capability increases when enriched with B_{10} isotope. Because of good thermal conductivity and thermal shock resistance, composite materials containing boron carbide have been proven to be suitable as a candidate material for the first wall of nuclear fusion reactors (Chkhartishvili et al., 2023).

On the other hand the low fracture toughness and poor sinterability characteristics of B_4C pose some limitations, mainly in achieving high-density and high-mechanical-strength composites. Thus, efforts are being directed toward improving the sintering behavior of B_4C with different additives to overcome such challenges (Heydari & Baharvandi, 2015). The maximum density that can be achieved after pressureless sintering of B_4C using additives is below 95% even at high temperatures such as approximately 2100 °C. Research shows that it is difficult to achieve full densification of B_4C materials without the use of sintering additives (Yang et al., 2021). Sintering additives (such as metals (Zhang et al., 2014; Zhu et al., 2020; Ebrahimi et al., 2016), borides (Wang et al., 2025; Zhao et al., 2022), oxides (Xu et al., 2024; Xiong et al., 2018) etc.) are added to B_4C powder to promote sintering.

*Sorumlu Yazar/Corresponding Author: Pelin Çağım TOKAT-BİRGİN e-posta/e-mail: pelincagim.tokat@dpu.edu.tr

One of the alternatıves to improve the sinterability characteristics of B_4C is spark plasma sintering (SPS). SPS technique is advanced enough to allow the production of composites with very high densities at temperatures significantly lower than those used in conventional sintering, and within extremely short periods of time, compared to what is required with other traditional techniques. The method fosters densification, as interparticle diffusion mechanisms are accelerated by applying electrical current and mechanical pressure, allowing for easy control of grain growth (Le Godec & Le Floch, 2023). Niu et al. used Flash Spark Plasma Sintering (FSPS) to densify B_4C ceramics and achieved 99.2% densification at 1931 °C under 15.3 MPa pressure with minimal grain growth. (Niu et al., 2016). There is no clear and comprehensive scientific research on B_4C–WC–Y_2O_3 composites produced directly by Spark Plasma Sintering (SPS), apart from a few indirect studies and one patent. A U.S.-based patent describes making a composite containing 70–95 percent B_4C, 2–15 percent WC, and 3–15 percent Y_2O_3, wherein such structures can achieve a level of about 90–99 percent theoretical density that may be attainable by high-temperature sintering at among the highest possible ranges, 1600 to 2600 °C (US Patent Application, 2020). B_4C–metal (W), WC–Co–B_4C, and WC–Y_2O_3 are among the composites described in the academic literature as obtained by using the SPS method. Özer (2015) revealed a value of 5.15 MPa·$m^{½}$ for fracture toughness from B_4C matrix composites containing 5-15 vol.% metallic W and consolidated by SPS (Özer, 2015). Another study provided results of relative density reaching 99.5% together with high hardness values for materials processed by SPS belonging to the class of WC–Co–B_4C systems (Lee & Park, 2021). High-density B_4C–TiB_2–SiC composites were formed through an *in situ* reaction between B_4C, Ti_3SiC_2, and Si. According to Pan Yin *et al.* (Yin et al., 2018), spark plasma sintering of the mixture at 1650 °C resulted in the formation of intergranular and intragranular structures containing various types of nanoparticles within the composite. A composite sample which contains 30wt%TiB_2+SiC has low density exhibited optimum mechanical properties comprising high flexural strength 531.2 MPa, good fracture toughness 5.77 MPam$^{1/2}$ and moderate microhardness 28.6 GPa (Li et al., 2025). In another study, researchers observed that adding 1% Y_2O_3 to binderless WC systems resulted in a relative density of 99.7% and fracture toughness of approximately 5.44 MPa·$m^{½}$ (Zhang et al., 2025).

Other works have proven that the material combination is promising, although it does not directly and comprehensively involve the B_4C–WC–Y_2O_3 via SPS. A composite structure, defined by a composition from a United States patent, consists of 70–95% B_4C, 2–15% WC, and 3–15% Y_2O_3. This study will observe how WC and Y_2O_3 additives influence of sinterability as well as the mechanical strength of B_4C-based composites. The present study will also provide a detailed description of phase transformations, densification behavior, and microstructural evolution induced within the B_4C matrix by these additives. More to this, an elaborate assessment of these composites' appropriateness in highly advanced engineering applications will be carried out.

2. Materials and Methods

The starting powders used were B_4C (Kent Chemistry, 99.5% purity), WC (Kent Chemistry, 99.9% purity), and Y_2O_3 (Bostonchem, 99.99% purity). These raw materials were weighed according to the stoichiometry given in Table 1. The prepared powders were mixed for 5 hours in an MMD brand Turbula mixer for homogenization. Subsequently, the mixtures were consolidated using an SPS2000 spark plasma sintering furnace. The samples were sintered at 1900 °C for 8 minutes under an argon atmosphere with an applied pressure of 40 MPa and a heating/cooling rate of 10 °C/min. A relatively low heating and cooling rate (10 °C/min) was used to minimize thermal stresses. The dimensions of the sintered samples were 10 mm in diameter and approximately 8-10 mm in thickness.

Table 1. Sample codes and volumetric proportions of raw materials used

Sample Name	B_4C (vol.%)	WC (vol.%)	Y_2O_3 (vol.%)
B1	100	-	-
B2	80	20	-
B3	80	17.5	2.5
B4	80	15	5

XRD patterns were obtained using a PANalytical X-ray diffractometer for phase analysis of the sintered samples. Cu and Ni radiation were used for the XRD analysis at 40 kV and 40 mA. The diffraction patterns were recorded using the 2θ range of 10° to 80° and a dwell time of 1 second per step. Scanning electron microscopy (SEM) analyses were carried out to determine the morphological properties of the raw materials and the phase distribution, grain size, and microstructural characterization of the composite samples after production. These examinations were performed using the SEM (FEI Nova NanoSEM 650). Vickers hardness analyses were conducted using the Shimadzu HMV device, applying a load of 1000 gf for 10 seconds, hardness measurements were taken from 5 different

locations on the surface and the results were converted to the GPa unit according to the following equation by taking the arithmetic averages:

$$H\ (GPa) = \frac{HV}{102} \quad (1)$$

Based on the hardness values obtained automatically using a microscope, K_{IC} values were calculated using equation 2 (Anstis Approach - Simplified). In the equation, HV is Vickers hardness (kgf/mm²) and a is crack radius (mm).

$$K_{IC} = 0.0028.HV.\sqrt{a} \quad (2)$$

3. Results and Discussions

SEM and SEM–EDS analyses were performed on the starting raw materials (B_4C, WC, and Y_2O_3), and the data obtained are presented in Figure 1. It was observed that the powder particles mostly has a submicron size distribution. In the EDS spectra, only the B and C elements were observed in Figure 1a, only the W and C elements in Figure 1b, and only the Y and O elements in Figure 1c, supporting the presence of each phase in the initial powders.

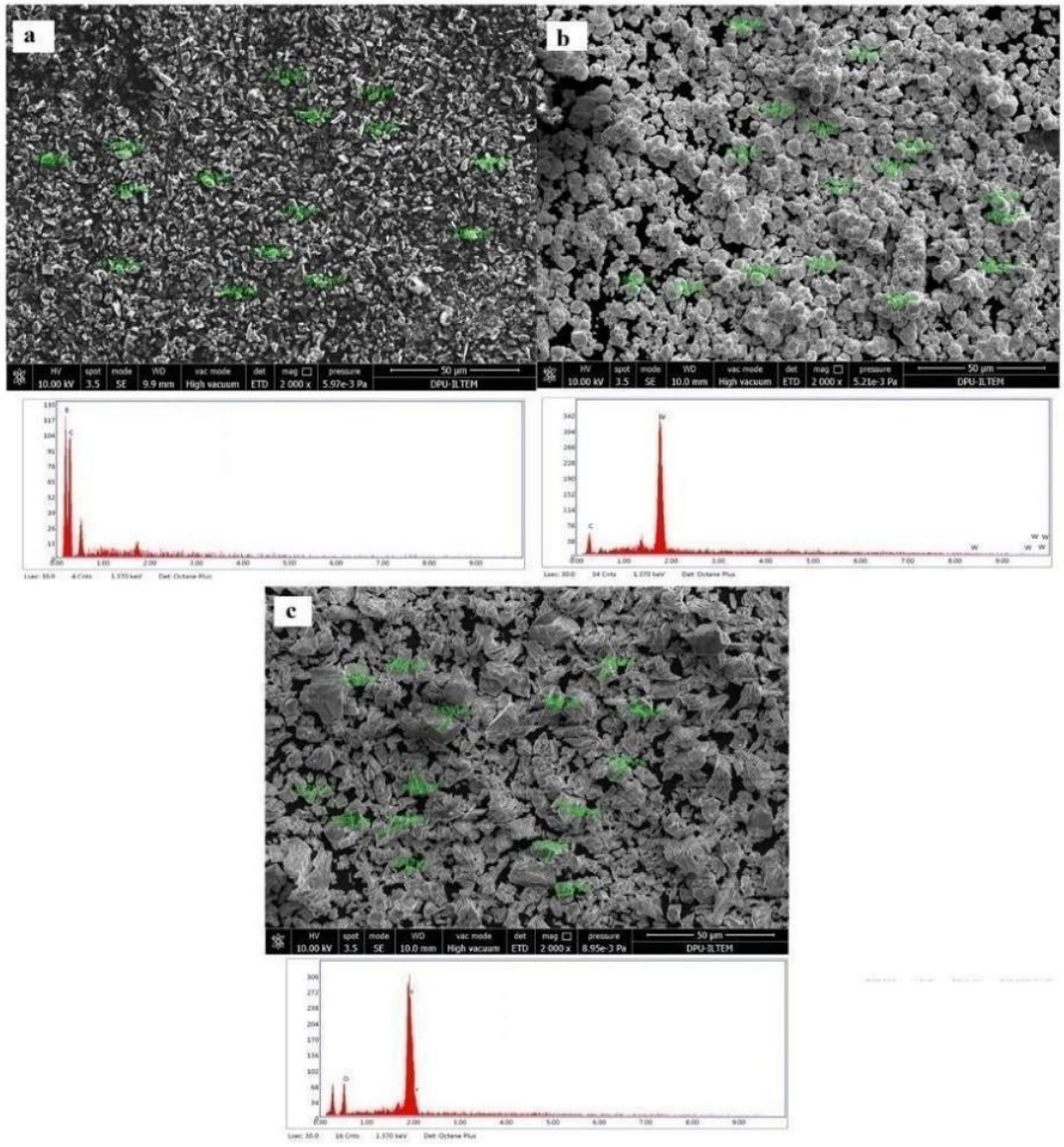

Figure 1. SEM micrographs of the raw powders: (a) B_4C, (b) WC, and (c) Y_2O_3.

XRD patterns of the sintered samples are given in Figure2. Since B1 contains a single B_4C phase, the peak intensities are higher than the other samples. Peaks belonging to the WC phase with PDF card number 00-25-1047 were detected in samples B2, B3 and B4. When examining the patterns of samples B2, B3, and B4, peaks with angles of 38.8° and 39.7° are observed in the W_2C phase belonging to PDF Card No. 00-035-0776. Additionally, in these three samples, a peak detected at a 44.5° angle was identified as the W_2B_5 phase (PDF Card No: 00-038-1365). It is believed to form as a result of the reaction between tungsten (W) and boron (B) released during high-

temperature sintering due to the decomposition of the W_2B_5 phase, B_4C, and WC. At high temperatures, this reaction allows boron atoms to diffuse into the tungsten lattice, facilitating the nucleation and subsequent growth of the W_2B_5 phase. Similar studies in the literature have also reported the formation of the W_2B_5 phase (Wen et al., 2000). Y_2O_3 phase with PDF card number 00-041-1105 was detected in samples B3 and B4. The Y_2O_3 peak intensity increased/decreased depending on the Y_2O_3 ratio.

In the literature, studies on B_4C-sintered systems doped with Y_2O_3 report almost full densification (relative density up to ~99.99%) (Lee et al., 2021). When it comes to WC as reinforcement, prior hot pressing studies of B_4C-WC composites demonstrate that adding WC increases the relative density, and fracture toughness. This implies that WC does not dissolve within the B_4C matrix but rather continues to function as a reinforcing phase that contributes to mechanical performance (Cura et al., 2004). WC localizes current density in the SPS due to its high electrical conductivity; this effect is not seen with insulating additives such as ZrO_2 or Al_2O_3. This allows for higher density to be achieved in a shorter time (Rahimi & Baharvandi, 2017).

Y_2O_3 limits grain growth by forming fine oxide phases during sintering. This effect is evident with Al_2O_3 or ZrO_2 additions, but is often not as strong as the WC–Y_2O_3 synergy on densification (Lyu et al., 2020). Y_2O_3 forms a barrier phase that increases the stability of the B_2O_3 layer. This effect is observed in SiC additives via the SiO_2 layer, but stability is lower due to volatility at high temperatures (Zhang et al., 2025).

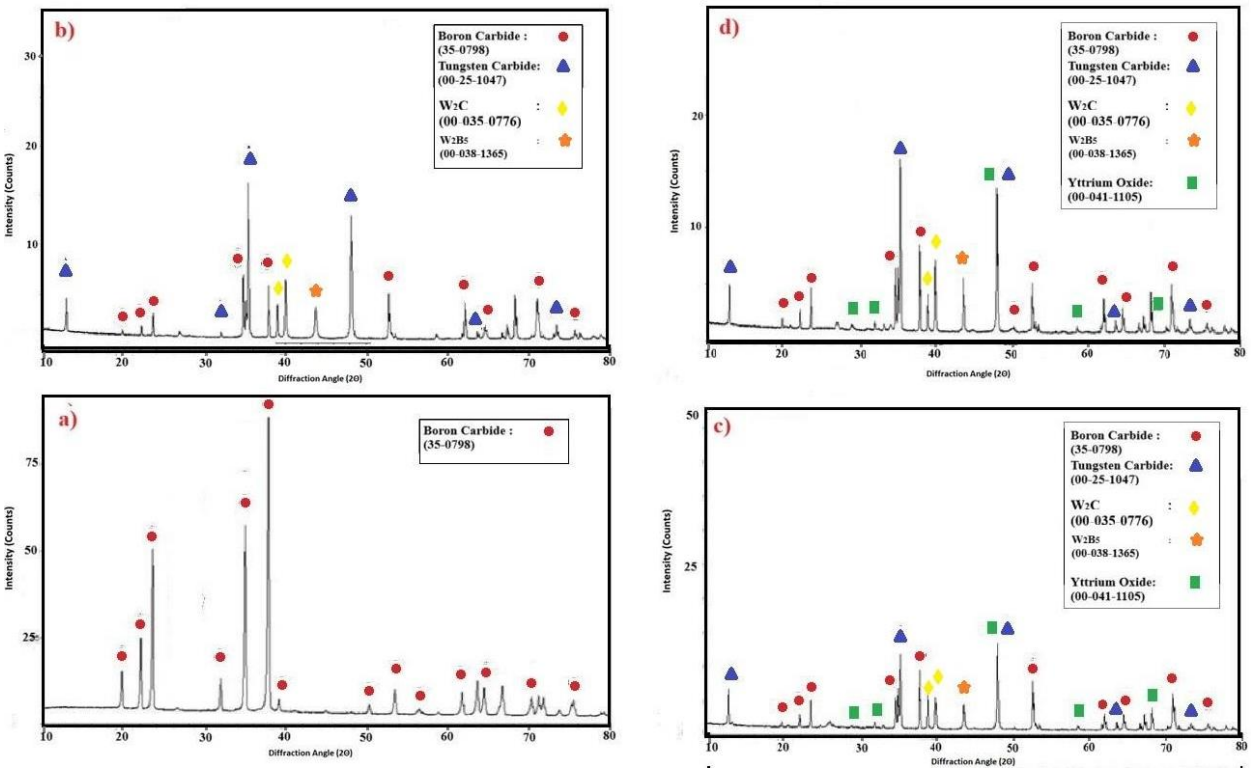

Figure 2. XRD graphs of the (a) B1 (b) B2, (c) B3 and (d) B4.

Figure 3 shows the theoretical, experimental, and relative densities of B_4C-based composite samples. Studies in the literature indicate that the SPS production method significantly increases the relative densities of the samples (Le Godec & Le Floch, 2023; Niu et al., 2016; Özer, 2015). With the advantage of the selected production method, relative densities in the range of 97.2-98.5% were obtained. The relative density values of the samples ranged from 97.2% to 98.7%, and the average relative density was calculated to be 98.03 ± 0.70%. Since WC and Y_2O_3 have high densities, the addition of these additives to the samples increased the theoretical densities. The fact that the experimental densities are very close to the theoretical values indicates that the samples were well sintered. The highest experimental density was obtained in sample B2 (80% B_4C + 20% WC), and the lowest density belonged to sample B1 (100% B_4C). Relative density decreased with the addition of WC. The addition of Y_2O_3 led to increased density. A slight increase in relative density was observed in the samples where the amount of Y_2O_3 increased (from B2 to B4), which is associated with the positive effect of Y_2O_3 reinforcement on density. Overall, the high relative density values confirm that the SPS method is a suitable method for densification of B_4C-based composites containing multi-phase additives.

Vickers hardness (GPa) and fracture toughness ($MPa.m^{1/2}$) data of the samples are available in Fig.4. The hardness data of the samples were 19.8 GPa for sample B1, 22.4 GPa for sample B2, 22.7 GPa for sample B3, and 23.5 GPa for sample B4, with an average hardness of 22.1 ± 1.6 GPa. Fracture toughness values of the specimens are 7 $MPa.m^{1/2}$, 8.7 $MPa.m^{1/2}$, 8.1 $MPa.m^{1/2}$, and 7.8 $MPa.m^{1/2}$, respectively, with an average value of 7.9 ± 0.7 $MPa{\cdot}m^{1/2}$. In the measured hardness values, it is observed that the addition of WC increases the hardness value compared to sample B1. The addition of Y_2O_3 also increases the hardness values in the same way. WC is a material with very high hardness, and its addition to composites has a positive effect on hardness values. Additives added to the B_4C matrix are generally evaluated in the literature to increase hardness and wear resistance, improve thermal shock and oxidation resistance, and facilitate densification by controlling grain growth. In this respect, the features of WC and Y_2O_3 compared to other additives in the literature are as follows: WC has a hardness of 23–29 Gpa (Wu et al., 2025), which is similar to TiB_2 (≈ 25 GPa) (Rubino et al., 2023) and significantly higher than SiC (≈ 20–22 GPa) and Al_2O_3 (≈ 18–20 GPa) (Perumal et al., 2025).

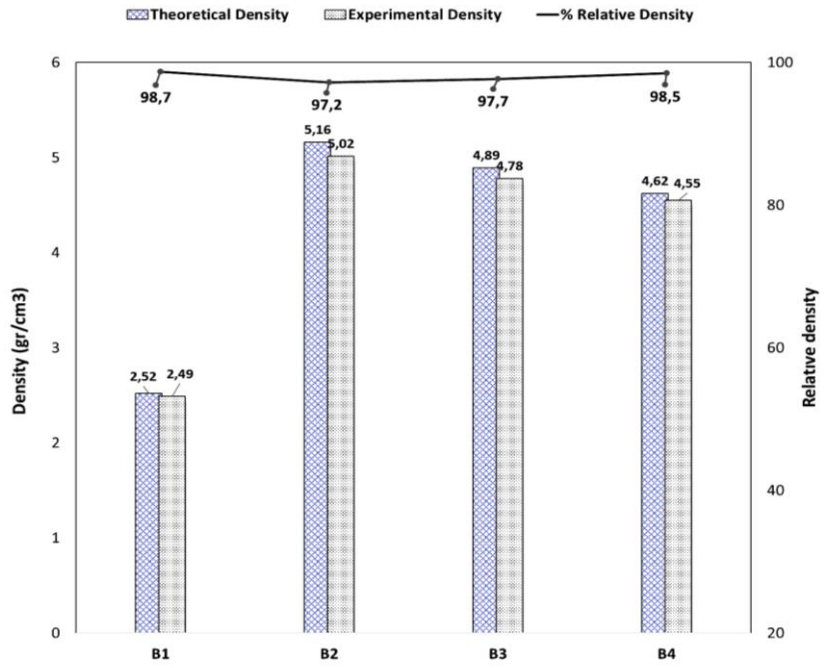

Figure 3. Theoretical, experimental and relative densities of B_4C-based composite samples.

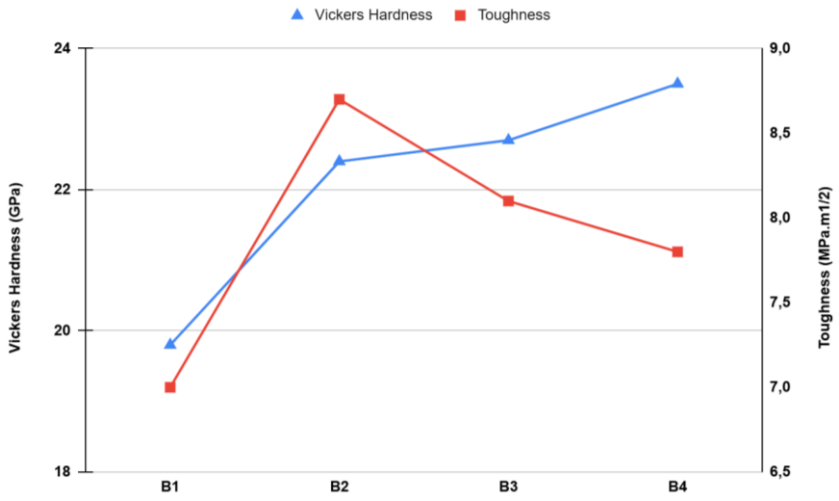

Figure 4. Hardness and fracture toughness values of B_4C-based composite samples.

Therefore, WC is one of the most effective additives for increasing the surface strength of B_4C. Numerous studies have reported that WC additives reduce the coefficient of friction and volumetric wear loss. The increases observed with SiC and Al_2O_3 additives are generally more limited. Therefore, WC additives are more significant, especially for surfaces subject to high wear. Even though WC is softer than B_4C, the rise in hardness we observe in the

composite doesn't come down to phase hardness alone. With WC addition, the material becomes denser, porosity drops, and the micro-structure tends to get finer and more uniform. All of this makes the material respond better to indentation, effectively offsetting the presence of the relatively softer WC and resulting in an overall increase in hardness. Y_2O_3 is generally used as a sintering aid because it increases sinterability and contributes to hardness by reducing porosity. In the combined effect (B3 and B4), the highest hardness can be achieved with both high density. In general, fracture toughness decreases as hardness increases. This classic trade-off between mechanical properties applies to many ceramic matrix composites. Hard materials have a more tightly bound structure at the atomic level, which prevents plastic deformation. As the deformation ability decreases, cracks propagate more easily, which reduces fracture toughness. However, this was not the case for B1 and B2. While the hardness increased with the addition of WC to B1, the fracture toughness also increased. In B3 and B4, it is clearly seen in the graph that there is a decrease in fracture toughness with the addition of Y_2O_3 and the reduction in the volume ratio of WC. For B3 and B4, the decrease in WC ratio caused a reduction in fracture toughness. The increase in fracture toughness observed with the addition of WC can be primarily attributed to the crack-bridging mechanism. WC particles, which are hard and have a high elastic modulus, interact with a crack propagating through the matrix and act as bridges between the crack surfaces. This bridging effect delays the complete separation of the crack surfaces, thereby increasing the energy required for crack propagation. In addition, the presence of WC particles can contribute to crack deflection by causing the crack path to become more curved and tortuous rather than straight. This situation extends the crack path, thereby increasing energy dissipation during fracture. When all these mechanisms are considered together, it can be concluded that the addition of WC enhances the composite's fracture toughness (Zhang, 2025).

In a composite containing Y_2O_3, the strength of the interfacial bond leads to improved mechanical properties. Y_2O_3 can alter the chemical structure of grain boundaries, reduce porosity by increasing density, and form or stabilize phases at the interfaces. These effects strengthen grain boundaries, thereby inhibiting inter-granular crack propagation and promoting fracture mechanisms that dissipate more energy. These effects contribute to stronger interfaces, which suppress inter-granular crack propagation and promote more energy-dissipating fracture mechanisms.

When parallel works on B_4C-based composites available in the literature are considered, WC contributes to hardness and wear resistance while Y_2O_3 contributes to oxidation resistance and grain boundary stabilization. In the present work, both WC and Y_2O_3 as additives embody these two mechanisms thereby resulting in improvement of the material. Therefore, despite the relative increase in the density of the produced material, the gains are considered significant, especially for engineering components that will operate in high wear loads and high-temperature environments.

The scanning electron microscope (SEM) images of the B1, B2, B3, and B4 samples produced with SPS are shown in Figure 5a, 5b, 5c, and 5d, respectively. Figure 5a shows the micro-structure of the pure B_4C sample (B1), and Figure 5b shows the micro-structure of the B2 sample, which was created by adding WC to the B_4C matrix. In the image in Figure 5b, the WC addition is clearly visible as sharp-edged light gray grains. The average size of these grains ranges from 30 to 60 µm. Figure 5c shows the micro-structure of sample B3, which contains Y_2O_3 and WC additions in addition to B_4C. It is noteworthy that the Y_2O_3 addition has a glassy appearance. Figure 5d shows the micro-structural analysis of sample B4, which contains WC and increasing amounts of Y_2O_3. With the increase in Y_2O_3 content, a significant increase in the number of Y_2O_3 particles in the matrix is observed. Due to the contrast difference arising from the atomic mass difference, WC grains appear darker in the image, while Y_2O_3 grains appear brighter and lighter in color. These findings demonstrate that the micro-structural morphology and distribution behavior of different additive elements can be successfully controlled.

Energy Dispersive X-ray Spectroscopy (EDS) analyses were performed on the produced B1, B2, B3, and B4 samples to determine the chemical composition and elemental distribution of the materials. Representative EDS spectra, taken from selected regions, are shown in Figure 6, with quantitative results in the table below. In the electron microscope image in Figure 6a, spot analysis was performed at two different locations with varying contrasts, and the results were similar, as expected. The mass percentage of B in the sample is in the range of 79-83%, while the C content is in the range of 16-20%.

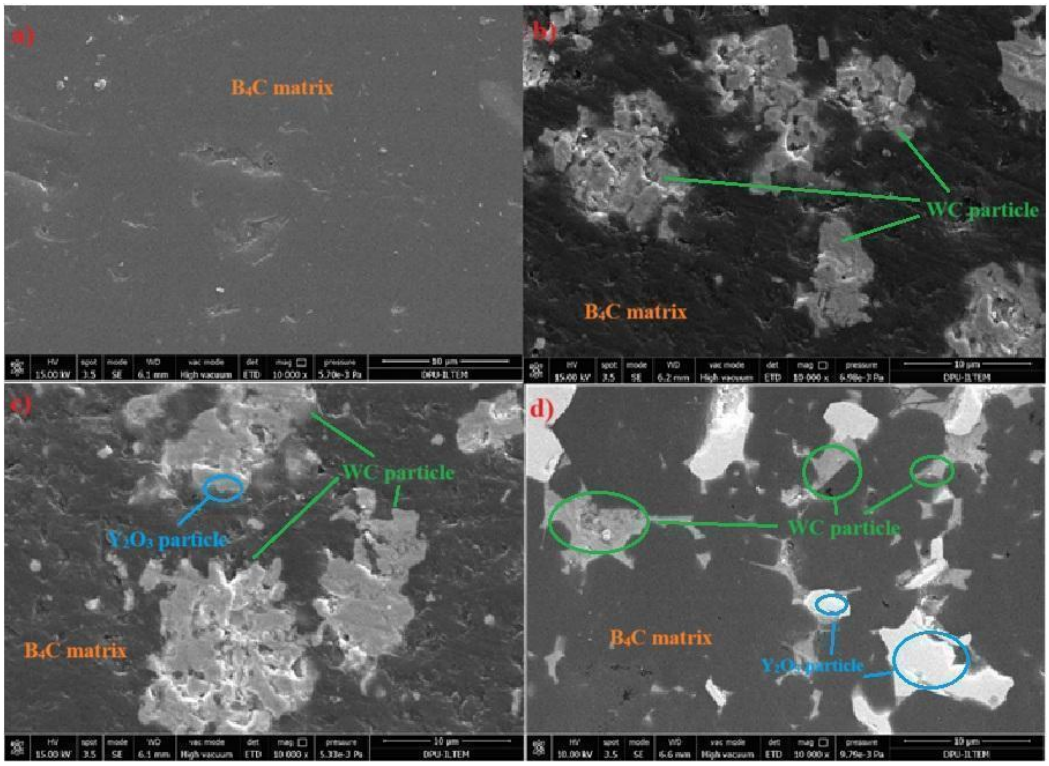

Figure 5. SEM images of samples a) B1, b) B2, c) B3, and d) B4.

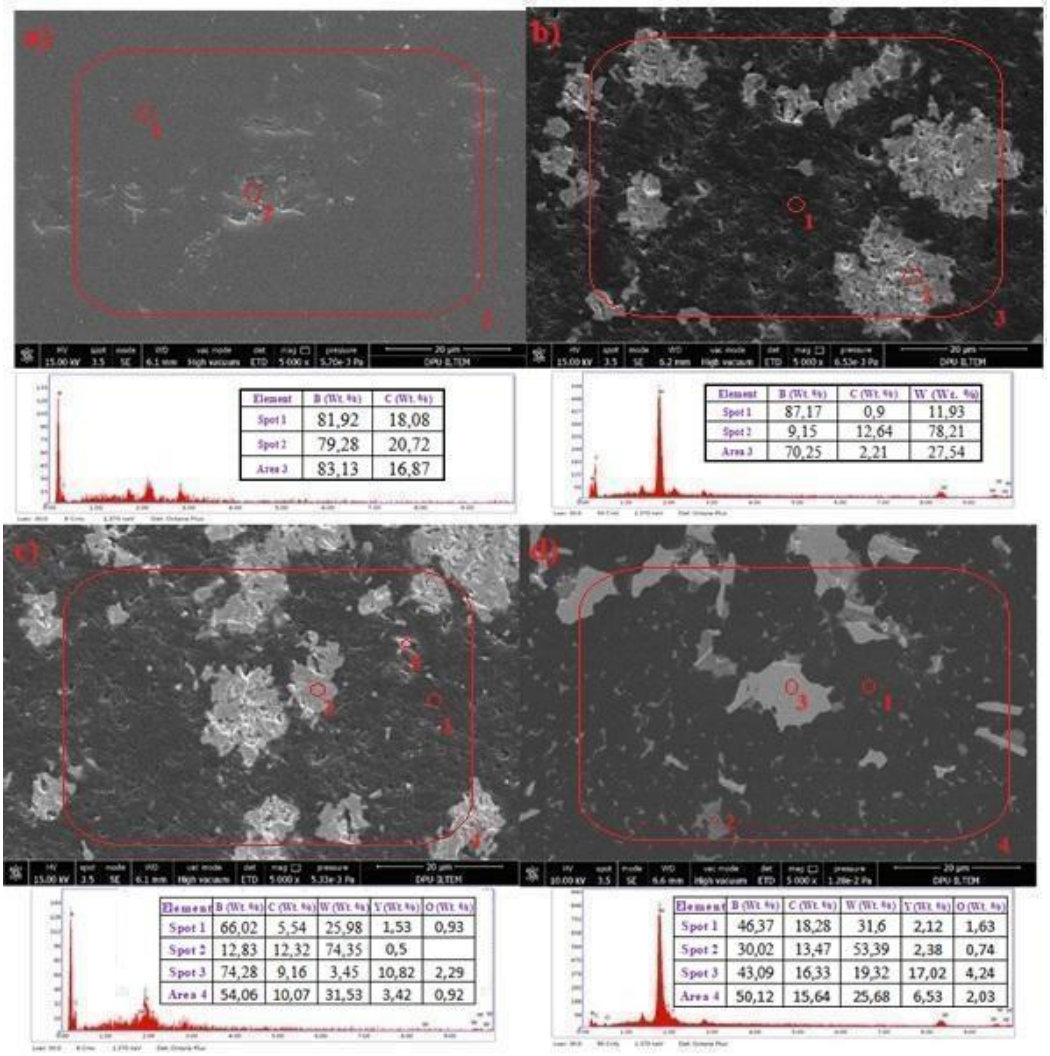

Figure 6. SEM-EDS analysis of the samples a) B1, b) B2, c) B3, and d) B4.

4. Conclusion

This study investigated the fabrication and characterization of the developed B_4C matrix WC/Y_2O_3 composites.

- X-ray diffraction (XRD) analysis confirmed the presence of the required phases after sintering, indicating successful phase formation.
- SEM and SEM-EDS analysis confirmed the reinforcement phases' distribution and size, as well as the constituent elements' distribution throughout the matrix.
- The measured physical and mechanical properties showed the effectiveness of the reinforcement: the relative density (%97.2- 98.7) was close to the theoretical value, indicating minimal porosity.
- The hardness test results showed a significant improvement compared to the base material, increasing up to 23.5 GPa, while the fracture toughness reached a value of 8.1 $MPa{\cdot}m^{1/2}$, indicating sufficient resistance to crack propagation.

The distinctiveness of the hardness values and their distribution close to theoretical values indicate that these composites exhibit high wear strength and sufficient mechanical degradation for fragmented cutting inserts, milling tools, and mold elements. The high efficiency achieved with the addition of WC particles is critically important for a long service life. The low-density, high-hardness advantage of B_4C, combined with its measured sufficient fracture toughness, makes the developed composites potential candidates for lightweight armor systems and ballistic protective plates. In conclusion, the obtained structural integrity, high stiffness, sufficient fracture toughness, and low porosity values demonstrate that the developed $B_4C–WC/Y_2O_3$ composites are not only suitable but also competitive and strategically essential materials for specific advanced engineering and industrial applications.

Declaration of Ethical Standards
The authors declare that they comply with all ethical standards.

Credit Authorship Contribution Statement
Author 1: Investigation, methodology, data interpretation; and writing—original draft.
Author 2: Investigation, methodology, writing—review and editing, and supervision.

Declaration of Competing Interest
The authors of this work declare that they have no conflicts of interest.

Data Availability Statement
All data generated or analyzed during this study are included in this published article.

Acknowledgements

We thank DPU-ILTEM for providing SEM and EDX analysis. We would like to express our gratitude to the T.R. Presidency of Strategy and Budget, project "Establishing the infrastructure for boron-based advanced technology ceramics laboratory," project number 2022K12-211404 for providing the laboratory equipment used in this study.

5. References

Chen, Y., Chung, Y. W., Li, S. Y. 2006. Boron carbide and boron carbonitride thin films as protective coatings in ultra-high density hard disk drives. *Surface and Coatings Technology*, **200**(12–13), 4072–4077. https://doi.org/10.1016/j.surfcoat.2005.02.164

Chkhartishvili, L., Makatsaria, S., Gogolidze, N., Tsagareishvili, O., Batsikadze, T., Mirzayev, M., Chedia, R. 2023. Obtaining boron carbide and nitride matrix nanocomposites for neutron-shielding and therapy applications. *Condensed Matter*, **8**(4), 92. https://doi.org/10.3390/condmat8040092

Cura, E., Şahin, F., Addemir, O., Radev, D. 2004. Microstructural and mechanical investigation of hot-pressed WC–Co/B_4C composites. Key Engineering Materials, 264–268, 1017–1020. https://doi.org/10.4028/www.scientific.net/KEM.264-268.1017

Ebrahimi, S., Heydari, M. S., Baharvandi, H. R., Ehsani, N. 2016. Effect of iron on the wetting, sintering ability, and the physical and mechanical properties of boron carbide composites: A review. International Journal of Refractory Metals and Hard Materials, 57, 78–92. https://doi.org/10.1016/j.ijrmhm.2016.02.007

Heydari, M. S., Baharvandi, H. R. 2015. Effect of different additives on the sintering ability and the properties of $B_4C–TiB_2$ composites. International Journal of Refractory Metals and Hard Materials, 51, 61–69. https://doi.org/10.1016/j.ijrmhm.2015.02.014

Le Godec, Y., Le Floch, S. 2023. Recent Developments of High-Pressure Spark Plasma Sintering: An Overview of Current Applications, Challenges and Future Directions Materials,16(3), 997 https://doi.org/10.3390/ma16030997

Lee, J. H., Park, H. K. 2021. Mechanical property evaluation of WC–Co–B_4C hard materials by a spark plasma sintering process. Korean Journal of Materials Research, 31(7), 397–402. https://doi.org/10.3740/MRSK.2021.31.7.397

Li, Y., Zhang, H., Wang, J., Chen, L. 2025. B_4C composites with Y_2O_3 addition fabricated by ultrafast high-temperature sintering. Journal of Alloys and Compounds, 984, 174157. https://doi.org/10.1016/j.jallcom.2025.183109

Lyu, X., Zhao, Z., Sun, H., Jiang, X., Hu, C., Song, T., Luo, Z. 2020. Influence of Y_2O_3 contents on sintering and mechanical properties of B_4C–Al_2O_3 multiphase ceramic composites. Journal of Materials Research and Technology, 9(5), 11687–11701. https://doi.org/10.1016/j.jmrt.2020.08.072

Niu, B., Zhang, F., Zhang, J., Ji, W., Wang, W., Fu, Z. 2016. Ultra-fast densification of boron carbide by flash spark plasma sintering. Scripta Materialia, 116, 127–130. https://doi.org/10.1016/j.scriptamat.2016.02.012

Özer, S. Ç. 2015. Production and characterization of boron carbide–tungsten-based composites using the spark plasma sintering (SPS) method. Thesis (M.Sc.). İstanbul Technical University, Institute of Science and Technology, Turkey.

Perumal, G., Senthilkumar, N., Naik, N. et al. 2025. Comparative assessment of the mechanical, tribological, and corrosion properties of Al/SiC/Al2O3 and Al/SiC/TiO2 hybrid composites. Discover Applied Science, 7, 237. https://doi.org/10.1007/s42452-025-06687-x

Rahimi, A., Baharvandi, H. 2017. Effect of tungsten carbide nanoparticles on mechanical properties and sinterability of B_4C–WC nanocomposites using pressureless sintering method. International Journal of Refractory Metals and Hard Materials, 66, 220–225. https://doi.org/10.1016/j.ijrmhm.2016.10.024

Rubino, F., Rotella, G., Perrella, M. et al. 2023. Microstructural and Mechanical Properties of Al2O3 and Al2O3/TiB2 Ceramics Consolidated by Plasma Pressure Compaction. J. of Materi Eng and Perform 32, 4391–4403. https://doi.org/10.1007/s11665-022-07403-1

Shin, S. J., Bayu Aji, L. B., Engwall, A. M., Bae, J. H., Taylor, G. V., Mirkarimi, P. B., Aracne-Ruddle, C., Nguyen, J., Kong, C. W. N., Kucheyev, S. O. 2023. Ultrathick boron carbide coatings for nuclear fusion targets. Fusion Science and Technology, 79(7), 841–852. https://doi.org/10.1080/15361055.2023.2194238

Schmidt, R. L. 2023. Cold spray of functionally graded aluminum metal matrix composite coatings reinforced with boron carbide and boron nitride nanotubes. Master's Thesis, Naval Postgraduate School Monterey CA,Virginia94.

US Patent Application (2020). High strength boron carbide ceramic material and method of making the same. US Patent Application No. 20200172441 A1

Wang, Y., Meng, T., Wang, G., Zhang, Y., Qin, G., Xu, Y., Liu, F. 2025. Microstructures and mechanical properties of fast hot pressure sintered B_4C–SiC–NbB_2 composites using a novel Nb_2Si sintering aid. Ceramics International, 51, 24, 41264-41271. https://doi.org/10.1016/j.ceramint.2025.06.350

Wen, G., Li, S. B., Zhang, B. S., Guo, Z. X. 2000. Processing of in situ toughened BWC composites by reaction hot pressing of B_4C and WC. Scripta Materialia, 43, 9, 853-857. https://doi.org/10.1016/S1359-6462(00)00502-9

Wu, C., Li, Y. K., Wan, C. L. 2020. Reactive-sintering B_4C matrix composite for armor applications. Rare Metals, 39(5), 529–544. https://doi.org/10.1007/s12598-020-01404-6

Wu, Z., Ye, N., Zhuo, H., Mao, J., Zhu, W., Gong, Z., & Tang, J. 2025. High-pressure and high-temperature synthesis of binderless nanocrystalline WC cemented carbide: Microstructure and mechanical properties. Ceramics International, 51(6), 7756-7765. https://doi.org/10.1016/j.ceramint.2024.12.213

Xiong, Y., Du, X., Xiang, M., Wang, H., Wang, W., Fu, Z. 2018. Densification mechanism during reactive hot pressing of B_4C–ZrO_2 mixtures. Journal of the European Ceramic Society, 38(12), 4167–4172. https://doi.org/10.1016/j.jeurceramsoc.2018.05.016

Xu, Z., Zhou, X., Peng, K., Yuan, T., Li, R., Zhou, Z. 2024. High-performance B_4C–Al_2O_3 composite ceramics fabricated via fast hot-pressing sintering. Materials Today Communications, 39, 108941. https://doi.org/10.1016/j.mtcomm.2024.108941

Yang, M., Zhuang, Y., Xing, P. 2021. High-performance B_4C–LaB_6 composite ceramics fabricated via hot-pressing sintering with La_2O_3 as sintering additive. Ceramics International, 47(23), 32675–32684. https://doi.org/10.1016/j.ceramint.2021.08.164

Yin, S. P., Zhang, Z. H., Cheng, X. W., Su, T. J., Hu, Z. Y., Song, Q., Wang, H. 2018. Spark plasma sintering of B_4C–TiB_2–SiC composite ceramics using B_4C, Ti_3SiC_2 and Si as starting materials. Ceramics International, 44(17), 21626–21632. https://doi.org/10.1016/j.ceramint.2018.08.245

Zhang, R., Liang, Y., Liu, H., Zhou, M., Zhang, X. 2025. B_4C composites with Y_2O_3 addition fabricated by ultrafast high-temperature sintering. Journal of Alloys and Compounds, 183109. https://doi.org/10.1016/j.jallcom.2025.183109

Zhang, Y., Wei, J., Li, X., Miao, Z., Hou, J., Wang, P., ... & Zhang, K. 2025. Sintering, toughening mechanism and amorphization of B4C-based ceramic composites: A review. Journal of the European Ceramic Society, 45(4), 117075. https://doi.org/10.1016/j.jeurceramsoc.2024.117075

Zhang, W., Yamashita, S., Kita, H. 2019. Progress in pressureless sintering of boron carbide ceramics – a review. Advances in Applied Ceramics, 118(4), 222–239. https://doi.org/10.1080/17436753.2019.1574285

Zhang, Z., Du, X., Li, Z., Wang, W., Zhang, J., Fu, Z. 2014. Microstructures and mechanical properties of B_4C–SiC intergranular/intragranular nanocomposite ceramics fabricated from B_4C, Si, and graphite powders. Journal of the European Ceramic Society, 34(10), 2153–2161. https://doi.org/10.1016/j.jeurceramsoc.2014.02.032

Zhao, J., Tang, C., Li, Q., Liu, Z., Ran, S. 2022. B_4C–TiB_2 composites fabricated by hot pressing TiC–B mixtures: The effect of B excess. Ceramics International, 48(9), 11981–11987. https://doi.org/10.1016/j.ceramint.2022.01.047

Zhu, Y., Luo, D., Li, Z., Wang, Y., Cheng, H., Wang, F., Chen, T. 2020. Effect of sintering temperature on the mechanical properties and microstructures of pressureless-sintered B_4C/SiC ceramic composite with carbon additive. Journal of Alloys and Compounds, 820, 153153. https://doi.org/10.1016/j.jallcom.2019.153153